

# Analytical Methods

Accepted Manuscript



This is an *Accepted Manuscript*, which has been through the Royal Society of Chemistry peer review process and has been accepted for publication.

*Accepted Manuscripts* are published online shortly after acceptance, before technical editing, formatting and proof reading. Using this free service, authors can make their results available to the community, in citable form, before we publish the edited article. We will replace this *Accepted Manuscript* with the edited and formatted *Advance Article* as soon as it is available.

You can find more information about *Accepted Manuscripts* in the [Information for Authors](#).

Please note that technical editing may introduce minor changes to the text and/or graphics, which may alter content. The journal's standard [Terms & Conditions](#) and the [Ethical guidelines](#) still apply. In no event shall the Royal Society of Chemistry be held responsible for any errors or omissions in this *Accepted Manuscript* or any consequences arising from the use of any information it contains.



Journal Name

ARTICLE

## Amine-rich Carbon Nanodots as a Fluorescence Probe for Methamphetamine Precursors

Tak H. Kim<sup>ab</sup>, Hiu Wai Ho<sup>c</sup>, Christopher L. Brown<sup>ac</sup>, Sarah L. Cresswell<sup>c</sup> and Qin Li<sup>ab\*</sup>

Received 00th January 20xx,  
Accepted 00th January 20xx

DOI: 10.1039/x0xx00000x

www.rsc.org/

Amine-functionalized carbon dots (A-CDs) were synthesized by one-step hydrothermal reaction of urea and citric acid. The purified CD sample exhibits a surface states dominated fluorescence emission with a quantum yield of 30%. The A-CDs demonstrate excellent sensitivity toward methamphetamine pre-precursor and precursor, and a remarkable selectivity against common drug cutting agents (diluent) such as Aspirin, Paracetamol, etc. The specific selectivity of CDs towards such type of drug precursor molecules is first time reported, which appears to be related to the spatial distribution of the surface functional groups. The fluorescence-based sensing mechanism is revealed by a detailed analysis on the static and dynamic fluorescence behaviour. We further demonstrated an immobilization strategy for fabricating solid-state sensors, and the retained sensitivity of the A-CDs after immobilization. The study reveals the potential of the use of a CDs as an effective sensing probe for illicit drugs, which is in demand.

### Introduction

The illicit drug market is a major source of profit for organized crime around the world. World production of amphetamine-type stimulants (ATS) such as methamphetamine have reached new levels with annual values now estimated at 144 tons globally and consumption appearing to be increasing in most regions in 2013. In 2013, it was estimated that 1.2% of the global population aged 15-64, or 54.81 million people, had used ATS (excluding the use of a related compound, ecstasy or MDMA (3,4-methylenedioxy-N-methylamphetamine))<sup>1</sup>. During illicit drug and clandestine laboratory investigations, a combined confirmatory test using gas chromatography mass spectrometry (GC-MS) is commonly employed for the identification and quantification of the manufactured drug compounds, their by-products and processing solvents to obtain tactical information and assist law enforcement agencies<sup>2, 3</sup>. Whilst these techniques are accurate with a detection limit of 0.1 µg mL<sup>-1</sup>, the samples typically require pre-processing in order to separate the target drug from diluent which is heavily cut with other white powder(s) such as glucose and/or caffeine. Several preparation steps are required in a typical quantitative analysis, which complicate the procedure, are costly and time-consuming<sup>4-6</sup>. Moreover,

these operations require access to dedicated test facilities. Overall, the current analytical process has limited instant response for the continuous investigation of suspicious samples and increases the chance of contamination and or data loss within the procedure.

To overcome these problems a quick colour-change presumptive test using direct analysis, such as the Marquis Test, is used in field to obtain a quick and simple test result<sup>7</sup>. Currently, the effectiveness of these tests on complex mixtures such as samples collected from a clandestine laboratory are limited; they tentatively give qualitative results but the presence of a wide range of substances may cause false positive results<sup>8, 9</sup>. Also, due to the destructive nature of presumptive tests, trace evidence samples are not examined this way. An accurate and direct analysis assay is highly desirable for clandestine drug law enforcement.

Carbon nanoparticles smaller than 10 nm, commonly dubbed carbon quantum dots or carbon nanodots (CDs), are carbogenic nanoparticles possessing surface functional groups such as hydroxyl and carboxyl moieties<sup>10-12</sup>. CDs have exhibited potential for a range of practical applications owing to their superior optical performance<sup>13</sup> and benign nature<sup>14, 15</sup>. In recent years, doped carbon nanodots synthesized by bottom up methods have been researched extensively due to the simplicity in preparation<sup>16</sup> and significant improvement in optical performance including quantum yield and optical tunability<sup>17, 18</sup>. As a consequence of doped CDs' versatility, they have been studied for wide range of applications including biological imaging<sup>19-22</sup>, light harvesting<sup>23</sup> and solid state lighting<sup>24-27</sup>. They have particular appeal in sensing applications, where they exhibit highly sensitive responses to target chemicals arising from their controllable surface functional groups and high quantum yields. Sensitive

<sup>a</sup> Queensland Micro- and Nano-Technology Centre, Griffith University, Nathan, QLD 4111, Australia.

<sup>b</sup> Environmental Engineering, Griffith University, Nathan, QLD 4111, Australia. Phone: +61 7 3735 7514 Email: qin.li@griffith.edu.au.

<sup>c</sup> School of Natural Sciences, Griffith University, QLD 4111, Australia.

† Footnotes relating to the title and/or authors should appear here.

Electronic Supplementary Information (ESI) available: [details of any supplementary information available should be included here]. See DOI: 10.1039/x0xx00000x

1  
2  
3  
4  
5  
6  
7  
8  
9  
10  
11  
12  
13  
14  
15  
16  
17  
18  
19  
20  
21  
22  
23  
24  
25  
26  
27  
28  
29  
30  
31  
32  
33  
34  
35  
36  
37  
38  
39  
40  
41  
42  
43  
44  
45  
46  
47  
48  
49  
50  
51  
52  
53  
54  
55  
56  
57  
58  
59  
60

detections of various metal ions<sup>28-33</sup>, hydrogen peroxide /glucose<sup>34</sup>, biothiols<sup>35, 36</sup>, chlorine<sup>37</sup>, pentachlorophenol<sup>38</sup> and norfloxacin<sup>39</sup> have been successfully demonstrated.

Here we report that CDs synthesized by a hydrothermal reaction of urea and citric acid are sensitive to methamphetamine precursors, namely phenylpropan-1,2-diol (PAC-diol) and phenylpropan-2-one (Phenylacetone, P2P), with an excellent selectivity particularly over the common drug cutting agents. Detailed static and dynamic fluorescence spectroscopy analyses were employed to elucidate the sensing mechanism. These CDs potentially provide benefits over the conventional methods of analysis as no complicated sample preparation for analyte detection is required and thus the analysis time can be considerably reduced. Moreover, it shows potential towards development into portable optical sensors and simple qualitative/quantitative test kits.

## Experimental

### Materials

Urea and citric acid were acquired from Chem-Supply Pty Ltd, Australia and used as received. The amphetamine sulfate was acquired from the National Institute of Measurement, Australia and other chemicals including acetaminophen, acetylsalicylic acid, caffeine, 4-aminobenzoic acid, 4-aminophenol, benzoic acid, benzyl alcohol, hydroquinone, 4-hydroxybenzoic acid, 4-methoxyphenol, fuchsin-basic, rhodamine B isothiocyanate, fluorescein isothiocyanate and (3-aminopropyl)triethoxysilane were obtained from Sigma Aldrich. Aniline was acquired from Alfa Aesar, glucose and sodium chloride were purchased from Chem-Supply Australia. All the above-mentioned drugs and chemicals were used without further processing or purification except 4-aminophenol which was dissolved into methanol and purified by the addition of activated carbon, stirring for 30 minutes followed by filtration. The resulting solution was dried under a stream of nitrogen. A pre-precursor of methamphetamine, phenylpropan-1,2-diol (PAC-diol) was obtained from the *L*-phenylacetylcarbinol process by using glucose and bread yeast. Subsequently, a precursor of methamphetamine, phenylpropan-2-one (Phenylacetone, P2P) was obtained by a pinacol-pinacolone rearrangement reaction on PAC-diol<sup>40,41</sup>.

### Preparation of CDs

Typically, 0.5 g of urea and 0.16 g of citric acid (molar ratio of 10:1) were dissolved into 10 mL of MilliQ water in a 30mL PTFE-lined autoclave. Then the autoclave was sealed and maintained at 180 °C for 24 hours. The autoclave was then cooled to room temperature and samples were collected for further processing. Dialysis membranes were acquired from Spectrum Laboratories, Inc. Dialysis was performed twice at different molecular weight cut-offs (MWCOs) for obtaining pure and mono-dispersed CD samples. Prior to dialysis, all the samples were filtered through 0.22 µm syringe filters in order to remove large aggregates then the filtrate was placed in a

MWCO 3.5 kDa membrane bag (the volume of each dialysis bag was prepared at 80 mL) and dialyzed against large amount of MilliQ water (20 mL of sample solution / 6 L of water for 36 hours, 500 mL of water was added every 2 hours and left for a further 12 hours). The 6 L of sample out of the 3.5 kDa bag was then condensed in a rotary evaporator to 60 mL and the condensed sample was placed in a MWCO 1 kDa membrane bag for further dialysis. The sample collected in the 1 kDa bag was named A-CDs.

### Solid sample fabrications

Solid samples were fabricated by drop casting A-CD solution on 10 mm circular coverslips. In order to immobilise the CD particles and disperse the CD sample evenly on the surface of the coverslips, (3-aminopropyl)triethoxysilane (APTES) was precoated onto the coverslips prior to CD sample casting. Initially the coverslips were sonicated in acetone and ethanol respectively and the coverslips were dried under nitrogen gas. 1mL of APTES were mixed with 20mL of ethanol and 40 µL of the diluted APTES were drop casted onto the cover slips and followed by drying at room temperature for 1 hr. Once the APTES was dried, the silane coated coverslips were washed with ethanol and 40 µL of A-CD sample solution was drop casted followed by drying for 4 hr at room temperature. The A-CD coated coverslips were finally washed with water to remove the access A-CDs on the coverslips and dried at room temperature.

### Characterisation

All the characterizations for this study were performed at room temperature. Atomic force microscopy (AFM) images were captured on a NT-MDT NTEGRA Spectra AFM by semi-contact mode. Transmission electron microscopy (TEM) images were captured on a Philips Tecnai 20 electron microscope operating at 200 kV. Hydrodynamic particle size and zeta potential were measured on a Malvern Zetasizer Nano ZS using dynamic light scattering (DLS) technique. X-ray photoelectron spectroscopy (XPS) spectra were acquired using a Kratos Axis ULTRA X-ray photoelectron spectrometer incorporating a 165 mm hemispherical electron energy analyser. Atomic concentrations and peak fitting was carried out using CasaXPS software. Fourier transform infrared (FTIR) spectra were recorded on a Perkin Elmer Spectrum Two FTIR spectrometer from 4000 to 750 cm<sup>-1</sup>. UV visible (UV-Vis) absorption spectra were measured on an Agilent 8453 UV-Vis spectrometer. Fluorescence emission spectra were recorded on a Thermo Scientific Lumina fluorescence spectrometer and fluorescent lifetime was recorded on an Edinburgh Photonics FLS920 fluorescence spectrometer with 377 nm pulse laser excitation source by using a Time-Correlated Single Photon Counting (TCSPC) technique and exponential tail fit analysis was used for the data interpretation. Quantum yields (QY) were calculated by comparing the integrated photoluminescence (PL) intensity values and the absorbency values with a reference sample<sup>42</sup>. GC-MS analyses of PAC-diol and P2P were carried out on a Perkin Elmer XL GC System using an Agilent HP-5MS capillary column (50 m × 0.33 µm) connected to a Perkin Elmer Turbo

Mass selective detector. The carrier gas was helium at a constant flow of 0.9 mL min<sup>-1</sup>. The front inlet was set to pulsed split mode with a split ratio of 25:1 and an injection volume of 0.5 μL. The injector temperature was set to 280 °C with an initial oven temperature of 100 °C held for 1 minute, then the temperature was increased at a rate of 30 °C min<sup>-1</sup> until 280 °C and maintained for 10 minutes. The mass selective detector operated between *m/z*= 41 and 450 in electron impact mode with an ionization energy of 70 eV. The MS database used for the identification of each sample was NIST MS Search 2.0 which is produced by the standard reference data program of the National Institute of Standards and Technology.

### Sensing tests

Tests in solution were carried out using 2 ml of the A-CD solution (concentration of 50 μg mL<sup>-1</sup>) and up to 0.2 mL of analyte stock solution, which was prepared in methanol at 1 mg mL<sup>-1</sup> concentration. Photoluminescence intensity was recorded as soon as the analytes were added and mixed by shaking the sample containing cuvette. Direct emission fluorometric methods were used for sensitivity and selectivity tests. 12 replicates of PAC-diol and P2P were run and the other samples were run in triplicate.

Solid-state sensing tests were performed by using A-CDs immobilized on 10 mm coverslips. The A-CDs coated coverslips were dipped into the analytes for 10 seconds followed by extraction and drying. Once the coverslips were dried, the solid samples were fixed on a solid sample holder and photoluminescence intensity was measured. Direct emission fluorometric methods were used and the samples were run in triplicate.

## Results and discussions

### Physicochemical properties

CD samples were synthesized by a hydrothermal process with urea and citric acid (10:1 molar ratio) in water at 180 °C for 24 hours. After the synthesis, the solution appeared as a brownish clear suspension with some dark sediment at the bottom. As described earlier, membrane dialysis was applied for isolation of A-CDs.

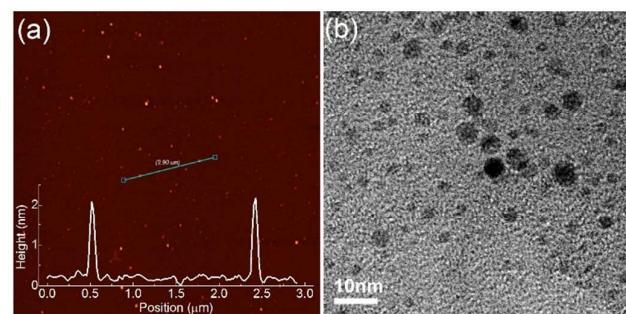


Fig. 1. (a) AFM (Inset: Size distribution obtained from DLS) and (b) HRTEM images of A-CD sample

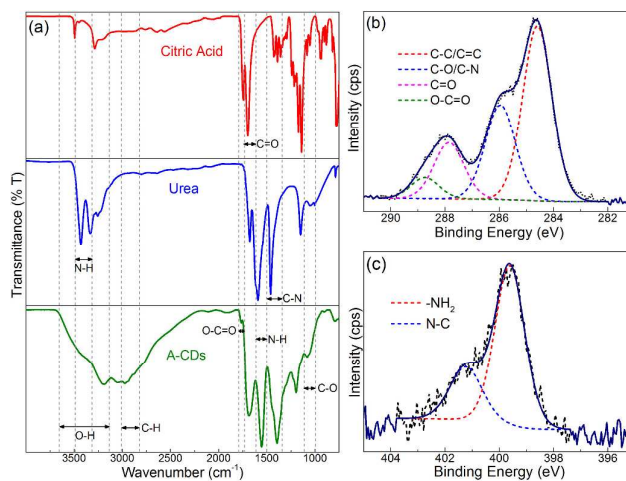


Fig. 2. (a) FTIR spectra of precursors and CD samples, (b) C1s and (c) N1s spectra of A-CDs

The A-CDs are colloidal stable showing no signs of aggregation, sedimentation or loss of photoluminescence (PL) intensity after being kept at room temperature for more than one year. As presented in Fig. 1 and Fig. S1, the presence of the nanoparticles and their narrow size distribution are confirmed by AFM, TEM and DLS characterizations. The dialysis membrane fractionation assisted to obtain mono-dispersed particles for A-CDs and the distribution in DLS shows size distribution between 1 and 3 nm with a peak at 2nm, which is consistent with the particle size of 2 nm as determined by AFM. The HRTEM image shows that the majority of the particles are smaller than 3 nm, however particles sized up to 8nm can be identified which may be attributed to particle aggregation during TEM sample preparation. Upon these CD particles, defined electron diffraction patterns cannot be obtained, indicating an amorphous carbon structure, consistent with other reported CDs<sup>20</sup>.

Analysis of A-CDs using FTIR (presented in Fig. 2 compared to citric acid and urea alone), reveals the surface functional groups on CD particles. The absorption bands at 3000 – 3500 cm<sup>-1</sup> are ascribed to stretching vibrations of –OH and –NH<sub>2</sub> groups. The peak at 1750 cm<sup>-1</sup> is assignable to the stretching frequencies of –C=O derived from –COOH. It is worth noting that the intensity of the N-H bending peak at 1549 cm<sup>-1</sup> is much stronger than the characteristic C=O stretching at 1655 cm<sup>-1</sup>, indicating the hydrothermal synthesis of urea and citric acid has resulted in abundant amino groups on the particle surface.

The XPS survey spectrum of A-CDs (Fig. S2) shows predominant O1s peaks at 531.4 eV, N1s peaks at 400.0 eV and C1s peaks at 284.6 eV, and identifies that A-CDs contain 58.4% C, 6.1% N and 35.5% O. It is interesting to note that although urea and citric acid were in 10:1 molar ratio as the starting reactants, there was only about 6% N in the CDs particles. This suggests that most of the urea may have been decomposed into ammonia gas under the reaction conditions, while citric acid formed the backbone of the CDs framework. It is known that pressurized ammonia gas can achieve both N

doping in the carbon conjugated structure<sup>31, 43</sup> and  $-\text{NH}_2$  attachment on the particle surface<sup>33</sup>.

The high resolution C1s spectrum shows that the CDs contain three different carbon bonding states; namely carbon-carbon bonds (C-C/C=C), carbon-oxygen bonds (C-O/C=O) and carbon-nitrogen bonds (C-N). The C1s peaks from the samples (Fig. 2) can be fitted into four peaks corresponding to  $\text{sp}^2$  C-C/C=C (284.6 eV), C-O/C-N (286.0 eV), C=O (287.8 eV) and O-C=O (288.6 eV)<sup>43</sup>. The high-resolution spectra of N1s reveal two peaks at 399.7 eV and 401.3 eV that correlate to  $-\text{NH}_2$  and graphitic N-C respectively<sup>27, 44</sup> which indicate amine functionalization on the surface as well as doped nitrogen in the carbon core.

Overall, both FTIR and XPS spectra suggest that in the hydrothermal reaction at 180°C, urea was first decomposed into ammonia and  $\text{CO}_2$ , whilst citric acid polymerized and carbonized into a carbogenic core<sup>45</sup>. These conditions resulted in the formation of carbon dots possessing surfaces richly functionalized by  $-\text{NH}_2$  and to a lesser extent  $-\text{COOH}$  groups. This preference for  $-\text{NH}_2$  functionality perhaps arises as a consequence of reactions/ interactions with decomposed urea.

In order to quantify the quantity difference between  $-\text{NH}_2$  and  $-\text{COOH}$  on the particle surface, A-CDs were reacted with Rhodamine B isothiocyanate (amine reactive) and basic-fuchsin (carboxyl reactive) and the amount of dye reacted with each group was quantified by spectrophotometric analysis using the absorption value and extinction coefficient of each dye molecule reacted with A-CDs (Experimental details and results are presented in Fig. S4 and Table S4). The results indicated that the amount of dye molecules linked on the amine of CDs (RhB-ITC, 2.4  $\mu\text{M}$ ) was 2.75 higher than the dye molecules attached on the carboxyl of CDs (fuchsin, 0.87  $\mu\text{M}$ ).

### Optical Properties

As presented in Fig. 3(a), obvious changes in UV-Vis absorption between as-synthesized and fractionated A-CDs were observed. The as-synthesized sample shows broad UV-Vis absorption with no distinctive peaks but a small shoulder peak at 310 nm, whereas the A-CDs show a distinctive absorbance peak at 310 nm with a slight shoulder peak at 350 nm. The absorption peaks are likely to arise from the  $n-\pi^*$  and  $\pi-\pi^*$  transition corresponding to C=O band and  $\text{sp}^2$  carbon core respectively<sup>46</sup>.

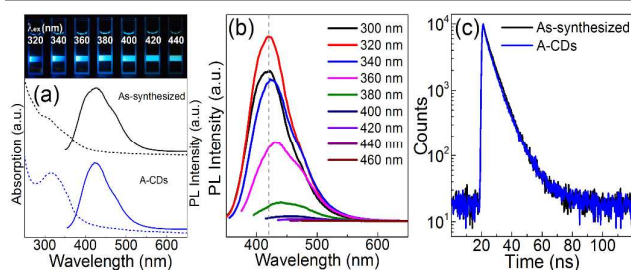


**Fig. 3.** (a) UV-VIS absorption (dotted line) and emission spectra at 340nm excitation, (b) Emission spectra of A-CDs and (c) fluorescence lifetime measured by TCSPC. Inset in (b) is an as-synthesized sample under different excitation energies.

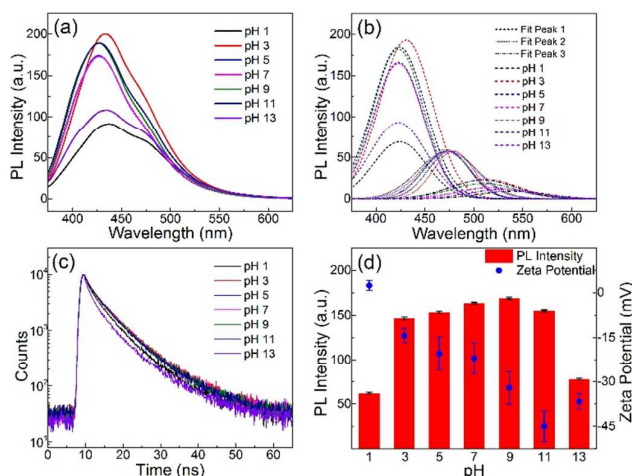


**Fig. 4.** pH effects on (a) photoluminescence, (b) Gaussian fitting of spectra (c) fluorescence lifetime decay and (d) intensity vs. zeta potential (measured vs. cumulative fit is presented in Fig. S5)

Photoluminescence (PL) emission spectra of A-CDs in Fig. 3 (b) show an almost excitation- independent emission with the maximum photoluminescence intensity recorded at 420 nm by 320 nm excitation. Excitation of the as-synthesized sample at the slightly longer wavelength of 340nm reveals somewhat different emission characteristics with the emission peak red shifting to 425nm with obvious shoulders at ~400 nm and ~480 nm. In comparison, the emission of A-CDs at 340 nm excitation shows narrower emission without an observable shoulder at ~400 nm and a less distinctive shoulder at ~480 nm. These distinctive emission properties most likely arise as a result of the much narrower size distribution as well as purer chemical composition. The emission excitation-independency demonstrates a surface states-dominated emission<sup>33</sup>. The quantum yield of A-CDs was characterized to be 30%.

Fluorescence decay of the samples was measured by Time-Correlated Single Photon Counting (TCSPC). The decay curves of the A-CDs and as-synthesized samples appear identical to each other as shown in Fig. 3 (c). They both can be fitted by a ternary-exponential function, indicating three emitting species. The PL lifetime constants of A-CDs were determined as:  $\tau_1=1.24$  ns (5%),  $\tau_2=5.38$  ns (76%) and  $\tau_3=11.51$  ns (19%). Among the various repeating measurements on A-CDs and as-synthesized dots, although there are slight differences between  $\tau$  values of each sample, fluorescence decay curves are all identical among the samples measured, which indicates that the lifetime of the samples may not be highly affected by their particle size or that the surface states of the particles are comparable among the samples.

A close inspection of the PL spectra of A-CDs reveals three split peaks. The differences among them becoming more apparent as the pH was varied (Fig. 4). The zeta potential of A-CDs was dramatically changed from 2.4 mV to -45.0 mV upon changing pH values from pH 1 to pH 13 as shown in Fig. 4(d) due to protonation and deprotonation of the carboxyl and amine functional groups on the surface of A-CDs. The photoluminescence intensity of A-CD samples shows

significant differences when measured at pH 1 and pH 13. However, the intensity at other intermediate pH levels (pH 3 to pH 11) shows reasonably stable levels which are noticeably different from CDs synthesized by different methods and precursors<sup>47-50</sup>. The emission spectra were further analysed by fitting the emission peaks to multiple Gaussian functions. In each case, a very good fit of the spectrum was obtained by decomposing into three Gaussian peaks. As presented in Fig. 4 (b), it is obvious that the first Gaussian peaks (dashed lines) contrast each other while the changes in the second Gaussian peaks (dotted lines) show minimum fluctuations. The surface emission may arise from a distribution of different emissive trap sites on A-CDs surface and the changes in the first Gaussian peaks are most likely caused by the surface state changes owing to protonation and deprotonation of the amine and carboxyl functional groups at the different pH levels. However, no significant changes in the second Gaussian peaks, regardless the pH levels, indicate that the emissions observed arise from the A-CDs core and are independent of pH. The changes in third Gaussian peaks (dash-dotted lines) are most likely caused by photon reabsorption as the changes correlate well with the changes of the first Gaussian peaks.

We further analysed the fluorescence dynamics of the A-CDs under different pH. The fluorescence decay curves in Fig. 4(c) show obvious deviations from the norm for pH 1 and pH 13. The decay curves can be fitted well by the tri-exponential function as displayed in Table S1. The three emission components indicate three different emissive sites, with a dominant component (~ 50 – 70%) of a lifetime constant around 4-5 ns, an intermediate component (~ 20-30%) of a lifetime constant around 10 ns, and a small population (~ 10%) of fast emissive species of a lifetime constant around 1 ns. The identified three components appear to match well with the three components identified by the static photoluminescence spectra. According to the photon counts percentage, we can associate the 4-5 ns component to the 1<sup>st</sup> Gaussian peak, the 10 ns component with the 2<sup>nd</sup>, and the fast emission with the 3<sup>rd</sup> Gaussian peak. When examining the lifetime change against pH (Table S1), it is obvious that at pH 3, A-CDs exhibit the longest lifetime, which seems to correlate well with its highest PL intensity at pH 3. Whereas at pH 1 and pH 13, the PL lifetime of A-CDs was significant reduced, and in the range of pH 5 to pH 11, the PL lifetime of A-CDs was slightly reduced compared to that under pH 3. Complete protonation of carboxyl at pH 1 and complete deprotonation of amine at pH 13 appears to have contributed to the charge transfer, which causes quenching and shortened PL lifetime.

Both the static and dynamic photoluminescence analysis suggests that the PL intensity change under different pH is caused by energy transfer due to the protonation and deprotonation of the amine and carboxyl surface functional groups<sup>51</sup>. The impact of pH change on the first Gaussian peak in both intensity and dynamics suggests that A-CDs exhibit surface states-dominated fluorescence.

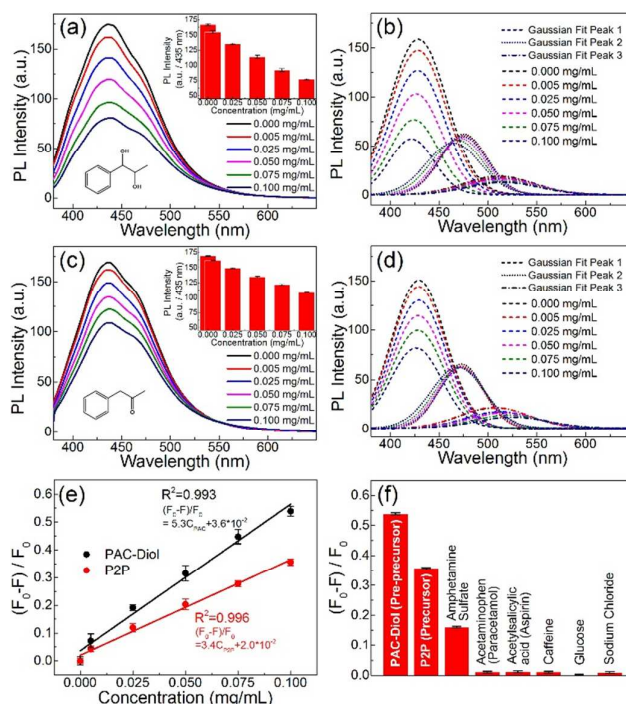


Fig. 5. Photoluminescence of CDs with (a) PAC-diol, (c) P2P, Gaussian fitting of CDs PL spectra with presence of (b) PAC-diol, (d) P2P (measured vs. cumulative fit presented in Fig. S5), (e) sensitivity and (f) selectivity of CDs at 0.1 mg mL<sup>-1</sup>

#### Sensitivity and selectivity to methamphetamine precursors

In order to assess the practicality of the prepared CDs as a sensor assembly, sensitivity and selectivity tests, against illicit drug precursors, amphetamine sulfate, commonly used diluents and a range of simple organic molecules were conducted using A-CDs. The precursors were prepared in a similar way to precursors produced from clandestine labs and they were all analysed by GC-MS prior to the sensitivity test. As presented in Fig. S3, all of the tested precursors contain impurities such as benzyl alcohol and benzoic acid which are inevitably produced during the process stages. These samples were tested without further purification since impurity levels in the precursor samples from clandestine labs may be comparable. Besides, purification of P2P might not be required in order to obtain methamphetamine as it (methamphetamine) can be isolated by crystallization of the final product after amination of P2P.

Sensitivity and selectivity of the A-CDs to methamphetamine precursors conducted at pH 7 is shown in Fig 5. The A-CDs show concentration-dependent sensitivities to the drug precursors as determined by fluorescence quenching tests. The A-CDs exhibit higher sensitivity to samples containing the drug pre-precursor (PAC-diol) than the sample of precursor (P2P). Photoluminescence intensity of A-CDs at 435nm was quenched by 54% when 0.1 mg (0.23  $\mu$ mol) of PAC-diol was introduced to 1 mL of A-CD solution, and by 36% when 0.1 mg (0.27  $\mu$ mol) of P2P was added.

The photoluminescence intensity of CDs is sensitive to the drug pre-precursors as the emission intensity decreases as the

concentration of the analytes increases and the responses from the samples are linear. Equation 1 describes the linear relationship between fluorescence and samples concentration.

$$(F_0 - F)/F_0 = m \times C + b \quad (1)$$

Where  $F_0$  and  $F$  are the photoluminescence intensity of A-CDs in the absence and presence of targeted molecules respectively,  $m$  is the slope,  $b$  is the intercept of the plot and  $C$  is the concentration of the sample in  $\text{mg mL}^{-1}$ . Table S2 summarizes the parameters for photoluminescence quenching plots. The standard deviation,  $\sigma$ , of 0.005 mg drug contained in 1 mL of CD samples, was calculated and from these data the lowest theoretical limit of detection may be estimated as  $2\sigma/m$  or  $3\sigma/m$  corresponding to confidence limits of 95.4% and 99.7% respectively<sup>52</sup>. Photoluminescence intensity of 12 replicates of sample drug containing A-CDs at  $5 \mu\text{g mL}^{-1}$  was measured and the standard deviation was derived accordingly. The theoretical detection limits were calculated to be  $2 \mu\text{g mL}^{-1}$  for PAC-diol and  $3 \mu\text{g mL}^{-1}$  for P2P at a confidence level of 99.7%. Any comparison with other direct detection methods was difficult as there is no established method or protocols for identification and quantification by a single instrument of such samples.

The closer assessment of the emission by multiple Gaussian functions in Fig. 5 (b) and (d) reveals that the photoluminescence quenching is obviously occurring to the first Gaussian peaks (dashed lines). This indicates that the photoluminescence quenching is a result of the analyte binding onto the CDs' surface functional groups, namely amine and carboxyl, causing charge-transfer induced quenching, sharing the same origin as pH induced quenching. The hydroxyl group on PAC-diol and the ketone group on P2P are both polar groups that would favourably interact with a protonated amine  $-\text{NH}_3^+$  or  $-\text{COO}^-$  via hydrogen bonding interactions. The fact that PAC-diol has two hydroxyl groups while P2P has only one ketone group explains the better sensitivity to PAC-diol.

Furthermore, by comparing the series of 2<sup>nd</sup> Gaussian peaks obtained from the sensing study presented in Fig. 5 (b) and (d), a slight quenching trend accompanied by a blue-shift of spectra maxima can be observed in A-CDs photoluminescence response to PAC-diol, but this is absent in response to P2P. This may be caused by an interaction between the PAC-diol phenyl ring with the carbon structure on A-CDs, arising when PAC-diol molecules lie flat on the particle surface, driven by the attraction of both hydroxyl groups to neighbouring amine or carboxyl moieties. On the other hand, it also suggests that the spatial distribution of these functional moieties complements the distance between the two PAC-diol hydroxyl groups.

In order to validate the quenching mechanism, the fluorescence lifetime and zeta potential of A-CDs in the presence of PAC-diol and P2P were investigated. The fluorescence decay data in Fig. 6 indicate that the lifetime of A-CDs was shortened by adding more analytes. All of the decay data can be fitted by a 3-exponential function as in the pH-

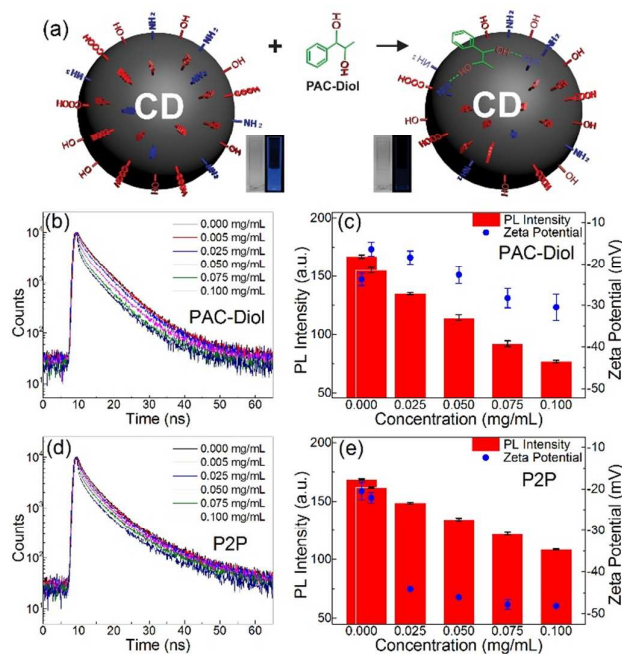


Fig. 6. (a) Potential interaction between CD's surface and PAC-diol, fluorescence lifetime decay, intensity and zeta potential changes by (b), (c) PAC-diol and (d), (e) P2P

dependency study. As presented in Table S3, there is a tendency of shortened lifetime in the three components when adding more analytes which correlates with PL quenching. This is likely due to charge transfer, which is accompanied by shortened PL lifetime<sup>42</sup>. The PL lifetime change is particularly noticeable in PAC-diol sensing, where the lifetime of the major emissive component was shortened from 5.30 ns to 4.18 ns when PAC-diol concentration increased from 0 to 0.1  $\text{mg mL}^{-1}$ . The change in the P2P system follows a similar pattern, but with a smaller amplitude, dropping from 4.64 ns to 3.98 ns.; The binding between CDs and the analytes can also be confirmed by noticeable changes in zeta potential values throughout the samples tested at each analyte concentration while the pH values of all the samples were kept constant at pH 6.8. The increased negative charge (from -23.8 mV to -30.5 mV as PAC-diol concentration increased) may suggest increased consumption of  $-\text{NH}_3^+$  due to its binding with the analytes.

A control test was performed using the solvent methanol (used for dissolving the analytes) as well as other common solvents including acetone, ethanol and propylene glycol (1, 2-propanediol). As presented in Fig. S6, no noticeable changes in PL intensity were observed which also supports that the quenching observed is due to the targeted analytes. However, propylene glycol showed 6% quenching which is most likely caused by binding of the diol to the surface of the CDs. The amount of quenching was comparably smaller than PAC-diol and P2P which further indicates that a phenyl ring in the targeted analytes plays an important role for the quenching observed.

An additional test was conducted with amphetamine sulfate, a similar illicit drug, and commonly used illicit drug

cutting agents (dilutents) including acetylsalicylic acid (Aspirin), acetaminophen (Paracetamol), caffeine, glucose, and sodium chloride<sup>52-54</sup> as analytes in order to assess the selectivity of the sample CDs to common materials as well as the feasibility of the illicit drug sensing application. Furthermore possible impurities found in the precursor samples and other chemicals which might be found and/or used for illicit drug production (4-aminobenzoic acid, 4-aminophenol, aniline, benzoic acid, benzyl alcohol, hydroquinone, 4-hydroxybenzoic acid, and 4-methoxyphenol) were tested under identical conditions. The results of these experiments are shown in Fig. 3(d), Fig. S7 and Table S5. They indicate that A-CDs were sensitive to none of the selected agents tested except amphetamine sulphate, which is of interest for further research and development into these systems. It is also worth noting that none of the impurities existing in the prepared precursors affects the sensitivity.

To summarise, as revealed by the FTIR and XPS in the previous section, the surfaces of A-CDs are predominantly covered by  $-NH_2$  moieties, which are likely to interact with the hydroxyl groups on PAC-diol and P2P through hydrogen bonding, leading to PL quenching. As illustrated by the scheme in Fig. 6a, the spatial distribution of  $-NH_2$  moieties on CDs surface appears to be important to an effective binding of the analytes, which explains the high selectivity towards PAC-diol and P2P, a pair of similar stereochemistry, different from the other tested organic molecules.

#### Solid state sensing

Solid-state sensing films were fabricated and tested against PAC-diol and P2P in order to demonstrate as a proof-of-concept sensing platform. A-CDs were immobilized on a glass substrate facilitated by APTES functionalization as illustrated by Figure 7(a). As shown by the photographs in Figure 7(b) and (c), the solid state A-CDs films remain emissive. When tested against PAC-diol and P2P, the solid-state A-CDs films showed concentration-dependent sensitivities similar to the quenching behaviour of suspended CDs. Same as the suspension tests, the solid A-CDs exhibit higher sensitivity to PAC-diol than P2P. Photoluminescence intensity of A-CDs was quenched by 42% at 0.1 mg of PAC-diol and quenched by 28% at 0.1 mg of P2P which were about 80% of the level of quenching by the CD suspension. This is most likely caused by reduced quantity of CD particles and limited exposed functional groups of the CD particles due to immobilization. Nevertheless this demonstrates a strong potential towards simple and portable sensing devices by utilising A-CDs.

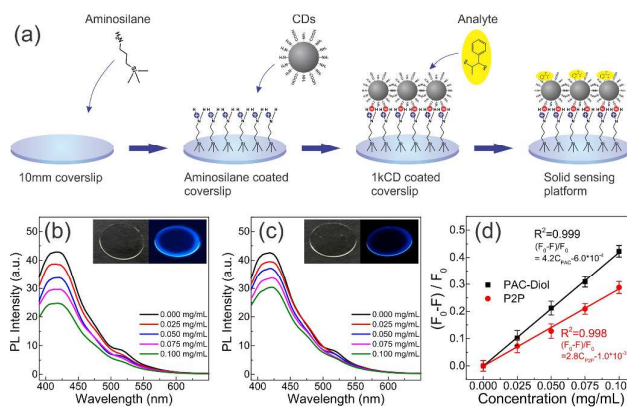


**Fig. 7.** (a) Solid sample fabrication and sensing strategy, quenching of the solid samples by (b) PAC-diol, (c) P2P and (d) sensitivity of the solid samples. Inset: solid sample pictures under room light (left) and 365nm UV light (right) (a) before and (c) after introducing PAC-diol

## Conclusions

Amine-functionalized CDs were synthesized in a one-step hydrothermal method by reacting urea and citric acid in water at 180°C. Chemical compositional characterization of the purified sample A-CDs shows a functional moieties-rich particle surface with  $-NH_2$  moieties in dominance. With a quantum yield of 30%, the A-CDs exhibit a significantly less excitation-dependent emission pattern, indicating a surface-states-dominated emission origin. Taking advantage of the high quantum yield and stable performance, a fluorescence sensing material for illicit drugs was demonstrated and the sample CDs show reasonable sensitivity toward methamphetamine precursors, namely PAC-diol and P2P. On the other hand, the CDs' photoluminescence intensity is not affected by commonly used drug cutting agents and solvents, which is highly favourable to practical applications. Such a specific selectivity of CDs towards a particular type of organic drug precursor molecule is first time reported, which appears to be related to the spatial distribution of the surface functional groups, the  $-NH_2$  moiety in particular. Detailed analyses on both static and dynamic fluorescence spectra were employed, which confirmed that surface-states dominated fluorescence provides an excellent platform for engineering chemical sensing devices. This study demonstrates the potential of CDs to function as effective sensing probes for presumptive testing and potential confirmatory testing for certain illicit drugs and the applicability of these materials for use in clandestine laboratory investigations.

## Acknowledgements

T. K. acknowledges the support of Australian Postgraduate Award and Queensland Smart Futures PhD Scholarship. Q.L. acknowledges a Griffith University Research Infrastructure Funding. The authors thank Dr Barry Wood at the University of Queensland for his assistance in XPS analysis, Mr. Shujun

Wang for acquiring the TEM images and Prof Paul McCormick at the University of Western Australia for helpful discussions.

## References

- United Nations Office on Drugs and Crime, *World Drug Report 2014*, United Nations, Vienna, Austria, 2014.
- Australian Crime Commission, *Australian Crime Commission Annual Report 2012-13*, Canberra Australia, 2013.
- Australian Government National Measurement Institute, *Illicit Drug Testing*, National Measurement Institute, Sydney Australia, 2005.
- M. E. Soares, F. Carvalho and M. L. Bastos, *Biomed. Chromatogr.*, 2001, **15**, 452-456.
- J. Trocewicz, *Journal of Separation Science*, 2001, **24**, 587-592.
- G. J. Mohr, M. Wenzel, F. Lehmann and P. Czerney, *Anal. Bioanal. Chem.*, 2002, **374**, 399-402.
- C. Anderson, *J. Chem. Educ.*, 2005, **82**, 1809-1810.
- A. R. W. Jackson and J. M. Jackson, *Forensic science*, Pearson/Prentice Hall, New York; Harlow, England, 2011.
- M. Hall, *False results put drug arrests under microscope*, USA Today, a division of Gannett Satellite Information Network, Inc, McLean, VA United States, 2008.
- S. N. Baker and G. A. Baker, *Angew. Chem. Int. Ed. Engl.*, 2010, **49**, 6726-6744.
- H. T. Li, Z. H. Kang, Y. Liu and S. T. Lee, *J. Mater. Chem.*, 2012, **22**, 24230-24253.
- L. Cao, M. J. Mezziani, S. Sahu and Y. P. Sun, *Acc. Chem. Res.*, 2013, **46**, 171-180.
- Y. P. Sun, X. Wang, F. Lu, L. Cao, M. J. Mezziani, P. G. Luo, L. Gu and L. M. Veca, *J. Phys. Chem. C*, 2008, **112**, 18295-18298.
- S. T. Yang, X. Wang, H. Wang, F. Lu, P. G. Luo, L. Cao, M. J. Mezziani, J. H. Liu, Y. Liu, M. Chen, Y. Huang and Y. P. Sun, *J. Phys. Chem. C*, 2009, **113**, 18110-18114.
- S. T. Yang, L. Cao, P. G. Luo, F. Lu, X. Wang, H. Wang, M. J. Mezziani, Y. Liu, G. Qi and Y. P. Sun, *J. Am. Chem. Soc.*, 2009, **131**, 11308-11309.
- F. Wang, S. Peng, L. Wang, Q. Li, M. Kreiter and C. Liu, *Chem. Mater.*, 2010, **22**, 4528-4530.
- Y. Yang, J. Cui, M. Zheng, C. Hu, S. Tan, Y. Xiao, Q. Yang and Y. Liu, *Chem. Commun.*, 2012, **48**, 380-382.
- Y. Dong, H. Pang, H. B. Yang, C. Guo, J. Shao, Y. Chi, C. M. Li and T. Yu, *Angew. Chem. Int. Ed. Engl.*, 2013, **52**, 7800-7804.
- Q. Li, T. Y. Ohulchanskyy, R. L. Liu, K. Koynov, D. Q. Wu, A. Best, R. Kumar, A. Bonoiu and P. N. Prasad, *J. Phys. Chem. C*, 2010, **114**, 12062-12068.
- R. Liu, D. Wu, S. Liu, K. Koynov, W. Knoll and Q. Li, *Angew. Chem. Int. Ed. Engl.*, 2009, **48**, 4598-4601.
- S. C. Ray, A. Saha, N. R. Jana and R. Sarkar, *J. Phys. Chem. C*, 2009, **113**, 18546-18551.
- S. Zhu, Q. Meng, L. Wang, J. Zhang, Y. Song, H. Jin, K. Zhang, H. Sun, H. Wang and B. Yang, *Angew. Chem. Int. Ed. Engl.*, 2013, **52**, 3953-3957.
- C. Wang, X. Wu, X. Li, W. Wang, L. Wang, M. Gu and Q. Li, *J. Mater. Chem.*, 2012, **22**, 15522-15525.
- F. Wang, Y. H. Chen, C. Y. Liu and D. G. Ma, *Chem. Commun.*, 2011, **47**, 3502-3504.
- T. H. Kim, F. Wang, P. McCormick, L. Wang, C. Brown and Q. Li, *J. Lumin.*, 2014, **154**, 1-7.
- X. Guo, C. F. Wang, Z. Y. Yu, L. Chen and S. Chen, *Chem. Commun.*, 2012, **48**, 2692-2694.
- W. Kwon, S. Do, J. Lee, S. Hwang, J. K. Kim and S.-W. Rhee, *Chem. Mater.*, 2013, **25**, 1893-1899.
- A. Zhu, Q. Qu, X. Shao, B. Kong and Y. Tian, *Angew. Chem. Int. Ed. Engl.*, 2012, **124**, 7297-7301.
- C. Hu, C. Yu, M. Li, X. Wang, J. Yang, Z. Zhao, A. Eychmuller, Y. P. Sun and J. Qiu, *Small*, 2014, **10**, 4926-4933.
- S. Yang, J. Sun, X. Li, W. Zhou, Z. Wang, P. He, G. Ding, X. Xie, Z. Kang and M. Jiang, *J. Mater. Chem. A*, 2014, **2**, 8660.
- Y. C. Lu, J. Chen, A. J. Wang, N. Bao, J. J. Feng, W. P. Wang and L. X. Shao, *J. Mater. Chem. C*, 2015, **3**, 73-78.
- W. Wang, T. Kim, Z. Yan, G. Zhu, I. Cole, N. T. Nguyen and Q. Li, *J. Colloid Interf. Sci.*, 2015, **437**, 28-34.
- X. M. Li, S. L. Zhang, S. A. Kulinich, Y. L. Liu and H. B. Zeng, *Sci. Rep.*, 2014, **4**, 4976.
- S. Liu, J. Q. Tian, L. Wang, Y. L. Luo and X. P. Sun, *Rsc Advances*, 2012, **2**, 411-413.
- L. Zhou, Y. Lin, Z. Huang, J. Ren and X. Qu, *Chem. Commun.*, 2012, **48**, 1147-1149.
- X. Ran, H. Sun, F. Pu, J. Ren and X. Qu, *Chem. Commun.*, 2013, **49**, 1079-1081.
- Y. Dong, G. Li, N. Zhou, R. Wang, Y. Chi and G. Chen, *Anal. Chem.*, 2012, **84**, 8378-8382.
- J. Li, N. Wang, T. T. Tran, C. Huang, L. Chen, L. Yuan, L. Zhou, R. Shen and Q. Cai, *Analyst*, 2013, **138**, 2038-2043.
- M. M. Yang, H. Li, J. Liu, W. Q. Kong, S. Y. Zhao, C. X. Li, H. Huang, Y. Liu and Z. H. Kang, *J. Mater. Chem. B*, 2014, **2**, 7964-7970.
- M. Cox, G. Klass and C. W. Koo, *Forensic Sci. Int.*, 2009, **189**, 60-67.
- K. A. N. Maroney, P. N. Culshaw, U. D. Wermuth and S. L. Cresswell, *Forensic Sci. Int.*, 2014, **235**, 52-61.
- J. R. Lakowicz, *Principles of Fluorescence Spectroscopy*, Springer US, 2006.
- V. H. Pham, H. D. Pham, T. T. Dang, S. H. Hur, E. J. Kim, B. S. Kong, S. Kim and J. S. Chung, *J. Mater. Chem.*, 2012, **22**, 10530-10536.
- X. Wang, C. Liu, D. Neff, P. F. Fulvio, R. T. Mayes, A. Zhamu, Q. Fang, G. Chen, H. M. Meyer, B. Z. Jang and S. Dai, *J. Mater. Chem. A*, 2013, **1**, 7920-7926.
- A. B. Bourlinos, A. Stassinopoulos, D. Anglos, R. Zboril, M. Karakassides and E. P. Giannelis, *Small*, 2008, **4**, 455-458.
- P. Yu, X. M. Wen, Y. R. Toh and J. Tang, *J. Phys. Chem. C*, 2012, **116**, 25552-25557.
- H. Liu, T. Ye and C. Mao, *Angew. Chem. Int. Ed. Engl.*, 2007, **46**, 6473-6475.
- Q. L. Zhao, Z. L. Zhang, B. H. Huang, J. Peng, M. Zhang and D. W. Pang, *Chem. Commun.*, 2008, **41**, 5116-5118.
- X. Jia, J. Li and E. Wang, *Nanoscale*, 2012, **4**, 5572-5575.
- P. C. Hsu and H. T. Chang, *Chem. Commun.*, 2012, **48**, 3984-3986.
- G. Blasse, *Mater. Chem. Phys.*, 1987, **16**, 201-236.
- C. J. Koester, B. D. Andresen and P. M. Grant, *J. Forensic Sci.*, 2002, **47**, 1002-1007.
- V. Puthaviriyakorn, N. Siriviriyasomboon, J. Phorachata, W. Pan-ox, T. Sasaki and K. Tanaka, *Forensic Sci. Int.*, 2002, **126**, 105-113.
- L. Poryvkina and S. Babichenko, *Detection of illicit drugs with the technique of Spectral Fluorescence Signatures*, eds. C. Lewis, D. Burgess, R. Zamboni, F. Kajzar and E. M. Heckman, Spie-Int Soc Optical Engineering, Bellingham, 2010, vol. 7838.